NEURAL NETWORK BASED UHVDC FOR ENHANCEMENT OF TRANSIENT COMPENSATION IN OFFSHORE WIND POWER PLANT

M.Sangeetha
Assistant professor
Department of Electrical and Electronics Engineering
Imayam College of Engineering
Kannanur,Thuraiyur -621206
sangee_maya@yahoo.co.in

R.Arivoli
Associate professor
Department of Electrical Engineering
Annamalai University,
Annamalai nagar- 608002
lnrarivolizc@yahoo.co.in

B.Karthikeyan
Professor and Head,
Department of Electrical and Electronics Engineering,
presidency university, Bangalore,
bcarthik@gamil.com

Abstract: *This paper presents a novel neural network controller improving compensation of transients and fast power transfer between a large scale offshore wind power plant and onshore high voltage direct current transmission (HVDC). The onshore HVDC is reconfigured with series and shunt compensators which named as unified-HVDC. In proposed work, the transient management scheme is done using DQ control technique. The compensation component is determined in such a way to minimize power oscillation and overshoots. The proposed control technique is analyzed using proportional integral (PI) controller and neural network controller. The test system is evaluated in MATLAB simulink environement.*

Key words: *Transient Compensation, Neural Network Controller, PI controller, HVDC, wind power plant, and DC link voltage.*

1. Introduction

Wind energy conversion systems have potential to fulfill the world's increasing energy demand. Generally, the generator of wind power plant (WPP) is based on either permanent magnet synchronous generator (PMSG) or doubly fed induction generator (DFIG) [1-5]. The more attention is given to PMSG based WPP because of its benefits of higher efficiency and it doesn't require gearbox [5-8]. The interconnection of wind power plant with grid system is done using back to back voltage source converters (VSCs). This ensures increased system reliability and cost efficient. The interconnection of such large scale offshore wind plant is carried out through high voltage direct current (HVDC) transmission system [9-13].

HVDC is a high power electronic technology which has been widely used in electric power system to transmit large amount of power for long distance [14-18]. Thus, the VSC-HVDC system provides independent control of active and reactive power flow in a transmission system. The important consideration during the bulk power transmission of HVDC system is grid fault disturbances which lead to stability problem. In [19-21] discussed about the performance of HVDC system and the significance of maintaining the system to be energetic during different fault conditions. The different configuration of VSC-HVDC system and its performance can be analyzed in [22-24]. From the discussion, it is found that the VSC- HVDC system configuration must provide fast fault detection and the large scale WPP should contains fault ride through capability [25-27]. This is achieved by implement proper control strategy of converter stations and many authors propose different control methodologies. The aim of the control technique is to enhance the fault ride through (FRT) capability of the system without affecting the wind power transfer and hence protect the entire system from severe fault disturbances. A new multilevel VSC – HVDC configuration is proposed in [28-30], but the system does not compensate the external grid fault.

This paper proposes series and shunt compensator named as Unified based HVDC system (UHVDC) with enhanced FRT capability. The proposed system has the series and shunt compensation devices to provide smooth power transfer, regulated dc link voltage, transient management and hence improved reliability. This can be possible by adopting DQ control technique. To reduce transient during fault, the proposed configuration utilizes neural network (NN) based control technique. This system proposes a comparison for proportional integral controller (PI) and NN based control. The proposed system assures to reduce the transients and dc link oscillation. This proposed large scale WPP with UHVDC system is designed and the results of different case studies are analyzed using MATLAB/ SIMULINK.

2. System configuration

The offshore WPP contains the PMSG based number of wind turbines connected either in series and shunt configuration [9]. the conventional HVDC system is based on thyristor valve for interconnection of two AC network. Generally classic HVDC link employed current source converter (CSC) for interconnection. However, the traditional HVDC transmission system has its own limitations such as larger in size hence requires large AC network [1]. Many researches are going on to overcome the conventional HVDC system by a voltage source current converter VSC-HVDC system.

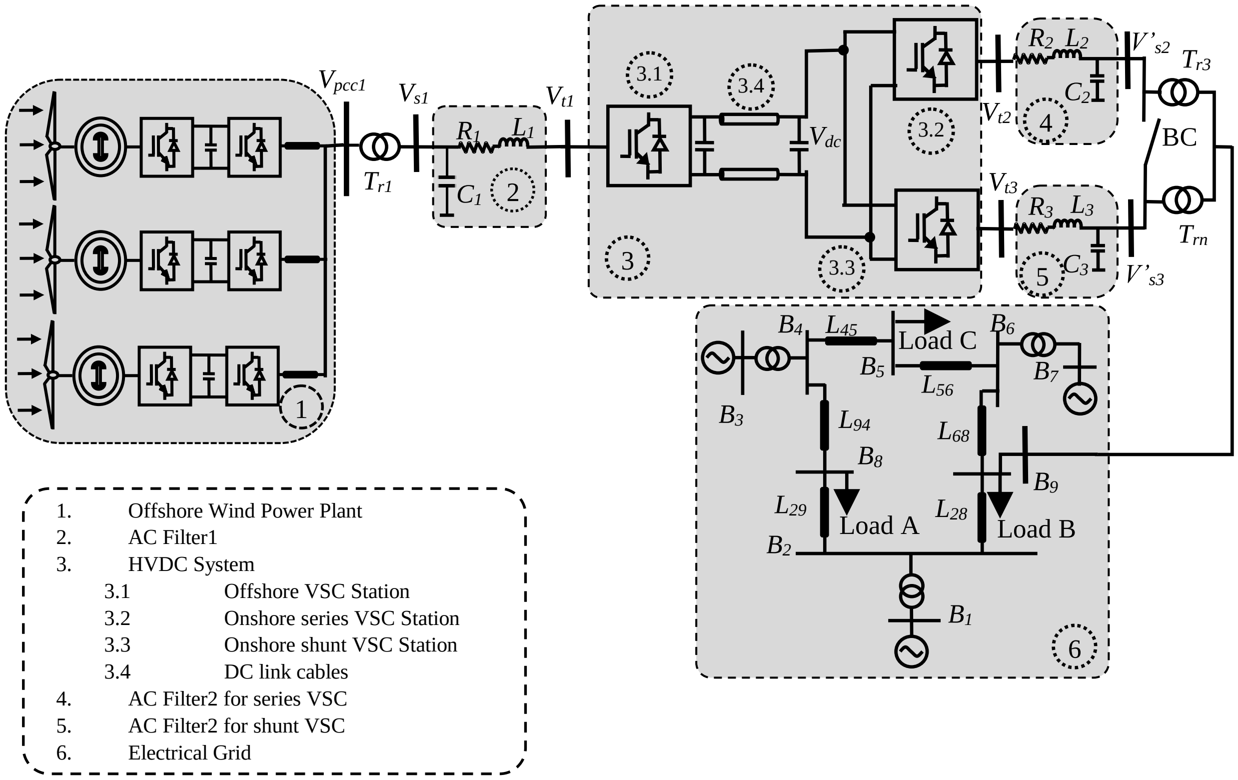

Fig.1. Configuration of VSC-HVDC connected to an IEEE-9 bus system

It employs modern semiconductor switches such as IGBT/GTO which is compact in size compared to classic thyristor valve based converters. It is based on self-commutated pulse width modulation (PWM) technology. Also, IGBT has the ability to turn ON and OFF with much higher frequency. Unlike conventional CSC based HVDC system the VSC-HVDC link does not requires any reactive power support [4, 24]. This VSC-HVDC system is suitable for changing the direction of power flow when the voltage is maintained in dc network. The different configurations of VSC-HVDC system is monopole, bipole, back-to-back or asymmetric, multi terminal [3] and [10, 26]. The Fig. 1 shows the system configuration of proposed multi-terminal VSC-HVDC system for wind power plant is connected to IEEE standard 9 bus system. The proposed configuration is called as UHVDC system which provides both series and shunt compensation. The WPP of proposed system has offshore and onshore VSC stations. The Offshore station accommodate one converter and the onshore station contains two independent converters namely series and shunt converters. The onshore VSC station is connected to the electrical grid system through two shunt connected transformers (Tr_3 and Tr_n).

The power produced by the WPP is transferred to the electrical grid system through this step-up transformer. The converters of both onshore and offshore stations should be capable to handle the power generated by the wind farms and the power is delivered to the electrical grid through HVDC system. In the Fig.1, B9 is the point of common coupling (PCC) where the HVDC and the electrical grid system is interconnected [8] and [11, 24]. The advantage of proposed configuration is to give series and shunt compensation to the system during any grid fault without requiring any additional compensation device. This helps to reduce the additional converter costs and hence the proposed system is a cost effective one.

If the fault is occurred in any one of the voltage source, the series transformer delivers the series voltage to prevent the entire system from the severe grid fault. If any fault occurs in V_{s2}, the transformer injects V_{ser} voltage at V_{s3} side so that the UHVDC system does not affected by any of the grid disturbances. Simultaneously, the proposed system provides voltage and current compensation by series and shunt VSC of onshore station. Similarly, if the fault is created at V_{s3} side, the series voltage is injected at V_{s2} side. The changeover from one operation into another during both steady state and transient condition is achieved by the proper handling of converter switches in UHVDC system [12, 29]. The operating principle of the proposed system is discussed in next chapter.

3. Mathematical modeling of proposed system

Fig 2 shows the equivalent circuit for proposed system, consists of two voltage sources V_{g1} and V_{g2}. The two voltage sources are connected to the grid through a series transformer Tr_{ser}.

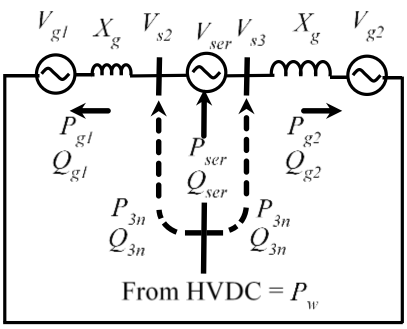

(a)

Fig. 2.a Equivalent circuit

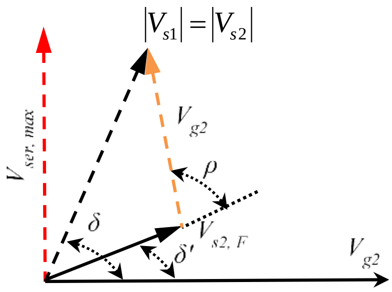

(b)

Fig. 2.b. Vector diagram for proposed UHVDC system

The flexibility of active and reactive power flow into the system is achieved with the help of this series transformer. The proposed system is like a simplified AC network. The two voltage sources consist of transmission impedances Z_{g1} and Z_{g2}. The series converter of proposed U-HVDC system is considered as a generalized voltage source represented as V_{ser}. From the Fig. 2(a), let us consider both the transmission impedances Z_{g1} and Z_{g2} contains pure reactance of same value X_g.

When the fault is created in any one of the AC grid either V_{g1} or V_{g2}, the series converter of UHVDC system provides compensation by injecting the required series voltage into the system. This causes the transmission line current flows though the series voltage source. Thus, the exchange of real and reactive power flow (P_{ser} and Q_{ser}) takes place between series transformer and transmission system. Where P_{ser} is the real power generated by the offshore wind power plant and the reactive power Q_{ser} is generated from the converter station. The total active power generated from the WPP is represented as *Pw*. It can be delivered by the series and shunt converters [30].

Let us assume the fault is created at V_{s2} side, there will be a voltage injection at V_{s3} side which causes the real and reactive power P_{3n} and Q_{3n} supplied at V_{s2}. This ensures the proper power transfer in the HVDC system during the grid fault condition [1] and [13]. The phasor diagram of proposed UHVDC system is shown in Fig 2(b). From the diagram, the voltage dip is occurred at V_{s2}, the fault voltage becomes $V_{s2,\,F}$ at an angle of δ'. To compensate this voltage dip, the required series voltage V_{ser} is injected through series transformer at V_{s3}. Thus, the real and reactive power flow at the voltage source V_{g2} can be formulated by the following equations,

$$P_{g_2} = \frac{V_{g2}}{X_g}\left[V_{s2,F}\sin\delta' + V_{ser}\sin\left(\delta' + \rho\right)\right] + P_{3n} \qquad (1)$$

$$Q_{g_2} = \frac{V_{g2}}{X_g}\left[V_{g2} - V_{s2,F}\cos\delta' + \frac{V_{ser}}{X_g}\cos\left(\delta' + \rho\right)\right] + Q_{3n} \qquad (2)$$

From the equation (1) and (2), the active and reactive power at V_{g2} is divided into three parts, that is, power due to fault voltage $V_{s2,\,F}$ power due to series voltage V_{ser} and the power flows takes place to the shunt converter of system.

$$P_{ser} - jQ_{ser} = \frac{V_{g2}}{X_g}\left[V_{ser}\sin\left(\delta' + \rho\right) - jV_{ser}\cos(\delta' \rho)\right] \qquad (3)$$

The equation (3) describes the separation of series active and reactive power. The rating of series converter is given by,

$$S_{ser,\max} = \sqrt{P^2{}_{ser} + Q^2{}_{ser}} = \frac{V_{g2}V_{ser,\max}}{X_g} \qquad (4)$$

For a fixed transmission line, the voltage source V_{g2} is maintained constant at 1 p.u and the reactance X_g is also considered as constant. The maximum voltage injected by the series converter during fault condition is $V_{ser,max}$. Thus the overloading capability of the proposed system is utilized more during FRT condition. This is accomplished by IGBT's of converters. Hence the FRT capability of proposed UHVDC system is enhanced. From the above analysis, many researchers concluded that the overloading capability of VSC is mostly preferable for a healthy transmission system [4, 14, 23].

4. Control scheme of onshore and offshore system

Here the control scheme of onshore and offshore VSC-HVDC system is discussed under steady state and faulted conditions. The onshore VSC is used to regulate dc link voltage. The offshore VSC is used to deliver the power generated from WPP and control the grid voltage. Conventional control structure of the system has fast inner current control loop and slower outer control loop [15, 26].

4.1 Control structure of shunt compensator

The control scheme of onshore and offshore shunt UHVDC system is shown in Fig. 3. From the figure, it is observed that there are four parts of the control scheme of shunt converter of UHVDC station. The first part is used to extract the negative sequence component and the second part performs computation of positive sequence component. The third part deals with transient detection and management scheme by either analytical or neural network (NN) method. The final part is the pulse generation part for shunt VSC.

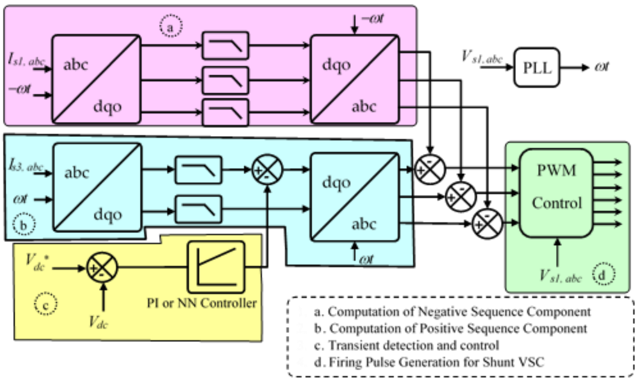

Fig.3. Control Scheme for onshore and offshore shunt VSC- HVDC system

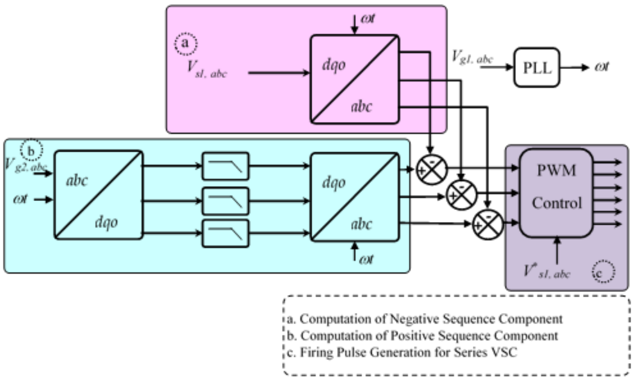

Fig.4. Control Scheme for series VSC of onshore WPP based UHVDC system

The positive and negative sequence (*dq0*) components of the shunt station is computed using positive and negative PLL angle ωt. The transformation is done from three phase (*abc* to *dq0*) to find out the positive and negative sequence (*dq0*) components. The *dq0* components are extracted directly from the voltage and current of the offshore station. The shunt VSC performs the current compensation and hence it deals with transformation of distorted three phase current to *dq0* quantities. Finally, the transformed reference current is given to pulse generation block to produce the required firing pulse of converter station [16, 24].

The general equation for three phase current in stationary axis (*abc*) is transformed into two phase rotating co- ordinates (*dq0*) is given below,

$$\begin{bmatrix} i_{Ld} \\ i_{Lq} \\ i_{L0} \end{bmatrix} = \begin{pmatrix} \cos\theta & \cos(\theta - \frac{2\pi}{3}) & \cos(\theta + \frac{2\pi}{3}) \\ \sin\theta & \sin(\theta - \frac{2\pi}{3}) & \sin(\theta + \frac{2\pi}{3}) \\ \frac{1}{2} & \frac{1}{2} & \frac{1}{2} \end{pmatrix} \begin{bmatrix} i_{sa}^* \\ i_{sb}^* \\ i_{sc}^* \end{bmatrix} \quad (5)$$

Finally, the desired reference current is calculated by taking inverse transformation of (*dq0*) axis into three phase (*abc*) rotating frame axis and is derived by the following equation (6).

$$\begin{bmatrix} i_{sa}^* \\ i_{sb}^* \\ i_{sc}^* \end{bmatrix} = \begin{pmatrix} \sin\theta & \cos\theta & \frac{1}{2} \\ \sin(\theta - \frac{2\pi}{3}) & \cos(\theta - \frac{2\pi}{3}) & \frac{1}{2} \\ \sin(\theta + \frac{2\pi}{3}) & \cos(\theta + \frac{2\pi}{3}) & \frac{1}{2} \end{pmatrix} \begin{bmatrix} i_{Ld} \\ i_{Lq} \\ i_{L0} \end{bmatrix} \quad (6)$$

4.2 Control structure of series compensator

Here the control strategy for series onshore UHVDC system is discussed and the diagram for the same is shown in Fig. 4. The series converter provides the voltage and transient compensation. When the fault is created at any one of the voltage source (V_{g1} or V_{g2}) the power transfer within the system is gets affected. To protect the WPP turbines based HVDC system from fault disturbances and severe transient, a series converter provides series voltage V_{ser}. This voltage is injected into the system at PCC through series transformer [17, 22] and [18, 21]. The equation for series voltage with phase angle is given below,

$$V_{ser}\angle\rho = V_{s3}\angle\delta - V_{s2F}\angle\delta \quad (7)$$

From the above equation, the positive sequence component of voltage magnitude and phase angle can be separated as,

$$|V_{ser}| = \sqrt{(V_{s3}\cos\delta - V_{s2,F}\cos\delta')^2 + (V_{s3}\sin\delta - V_{s2,F}\sin\delta')^2} \quad (8)$$

$$\rho = \tan^{-1}\left(\frac{V_{s3}\sin\delta - V_{s2,F}\sin\delta'}{V_{s3}\cos\delta - V_{s2,F}\cos\delta'}\right) \quad (9)$$

From the above expressions, the reference positive sequence voltage is determined by the pre fault grid voltage and measured grid voltage and is named as $V^{+}_{ser.dq,ref}$. When a fault is created at V_{s2} side, the compensation is done at shunt side V_{s3}. The total power delivered at series UHVDC system is given by the equation (10).

$$P_{tot,ser} = P_{ser} + P_{\cos}\cos(2\omega t) + P_{\sin}\sin(2\omega t) \quad (10)$$

The total active power $P_{tot,\,ser}$ is divided into three parts, series average power, cosine power and sine power and this power can be derived in equation (11) as given below,

$$\begin{bmatrix} P_{ser} \\ P_{\cos} \\ P_{\sin} \end{bmatrix} = \begin{pmatrix} I^{+}_{ser.d} & I^{+}_{ser.q} & I^{-}_{ser.q} \\ I^{-}_{ser.d} & I^{-}_{ser.q} & I^{+}_{ser.q} \\ I^{-}_{ser.q} & -I^{-}_{ser.d} & I^{+}_{ser.d} \end{pmatrix} \begin{bmatrix} V^{+}_{ser.d} \\ V^{+}_{ser.q} \\ V^{-}_{ser.d} \\ V^{-}_{ser.q} \end{bmatrix} \qquad (11)$$

From the above expression, $V_{ser,\,dq}$ and $I_{ser,\,dq}$ is the series voltage and current *dq* component. The sine and cosine terms of power is cancelled and equated to zero by the generation of reference negative sequence component of series voltage $V_{ser\text{-}dq,\,ref}$.

The negative sequence voltage component is obtained by solving the above equation and is written as below in equation (12).

$$\begin{bmatrix} V^{-}_{ser.d,ref} \\ V^{-}_{ser.q,ref} \end{bmatrix} = -\begin{pmatrix} I^{+}_{ser.d} & I^{+}_{ser.q} \\ -I^{+}_{ser.q} & I^{+}_{ser.d} \end{pmatrix}^{-1} * \begin{pmatrix} I^{-}_{ser.d} & I^{-}_{ser.q} \\ I^{-}_{ser.q} & -I^{-}_{ser.d} \end{pmatrix} \begin{bmatrix} V^{+}_{ser.d} \\ V^{+}_{ser.q} \end{bmatrix} \qquad (12)$$

Finally, the three phase voltages are given to pulse generation block to generate firing pulses for series VSC system.

5. Design of neural network controller

The neural network is an artificial intelligence tool used to formulate mapping between target data and input data. The procedure for training the neural network is shown in Fig. 5. Initial process is to collect the training data, i.e, input data and target data. This is the most important process, because it determines efficiency of neural network controller on compensation of transient and DC link voltage control [19]. The input data are error and integral error of DC link voltage and target data is compensation component of the current. DC link voltage error is the difference of reference and actual DC link voltage. Next process is the network creation, for this case two input and one output two-layer feed forward network is used. After neural network created, it must be configured for best network performance. The network configuration step consists of examining the input and target data, setting input and output sizes of the network to match the data and choosing an appropriate transfer function. After configuration, the weights of the two layers are initialized [20]. After trained and validation, the network is implemented in the simulation.

The simulation responses for neural network training are shown in Fig. 6. The total epoch is set to 1000 and best performance is reached at 608th epoch. From the obtained results it is observed that the output and target data are tracking well. Hence it is found the network is ready to implement in the simulation.

6. Simulation results and discussion

Simulation analyses on offshore WPP connected to power grid through UHVDC utilizing PI and proposed NN controllers are carried out in this section.

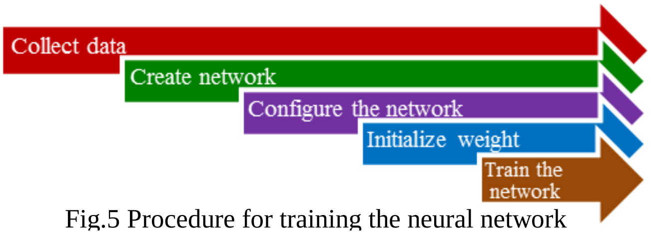

Fig.5 Procedure for training the neural network

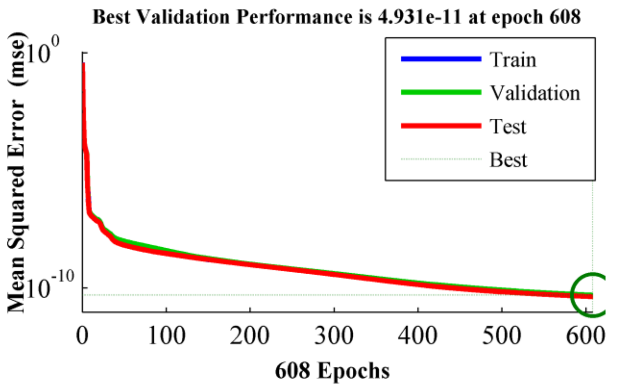

Fig. 6 Simulation response of performance of the neural network training

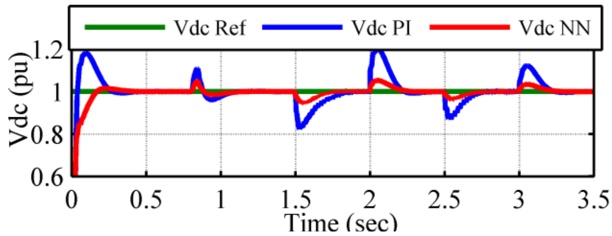

Fig.7 DC link Voltage control using PI and NN controllers

This section demonstrates the effectiveness of the proposed control technique for enhancing the compensation of transients and to provide fast power transfer under normal and faulted operating conditions. The voltage rating of the network is 230KV and the rating of HVDC is 250KVA which is equivalent to the offshore WPP. Parameter taken for simulation is given in table 2.

6.1 Analyze on DC link voltage control

The optimum compensation of transients and fast transfer of power between offshore WPP and power system network are determined by the finest control of DC link voltage of UHVDC at rated value. In this case study, the DC link voltage is controlled at 400KV using PI controller and proposed NN controller. The pu simulation result of DC link voltage control using PI and proposed NN controllers under WPP and grid sides disturbances are shown in Fig. 7. The operating conditions for this case study are fault injected in WPP at 0.8 sec, grid side faults are under voltage fault is injected between 1.5 sec to 2 sec and over voltage fault is injected at 2.5 to 3 sec. For initial condition, the peak overshoot of DC link voltage using PI controller is found to be 18.3% whereas 1.415% while using NN controller. Under WPP side fault condition, the peak overshoot of DC link voltage using PI controller is found to be 11% whereas 5% while using NN controller. Under grid side fault condition, the peak overshoot of DC link voltage using PI controller is found to be 20.5% whereas 4% while using NN controller. The performance of PI and NN controllers are analyzed and compared in table 1. This demonstration confirmed that the better minimization transients and better control of DC link voltage is achieved by the proposed NN controller.

6.2 Analyze on real power transfer using PI and NN controllers

Simulation analyses on real power transfer between offshore WPP and power system networks through UHVDC using PI controller and proposed NN controller are carried out in this section. The simulation results for control of real power transfer using PI controller and proposed NN controller under WPP and grid side faults are shown in Fig. 8.a and Fig. 8.b respectively. The operating condition for this case study is 10% voltage drop is injected in WPP from 0.6 sec to 1.2 sec and 10% voltage drop is introduced in power system network between 1.6 sec to 2.6 sec. The main objective of this investigation is to maintain real power at the second grid (P_{g2}) at 250 MW. The voltage drops in WPP created 0% power drop at first grid (P_{g1}) for without compensation. For maintaining P_{g2}, the series VSI injected series power (P_{sr}) 20% at point of common coupling there by P_{g2} is successfully maintained. While using PI controller, P_{g1} and P_{sr} have more peak overshoot and high oscillation. Whereas, NN controller P_{g1} and P_{sr} are successfully controlled with minimum oscillation and optimally regulated P_{g2}.

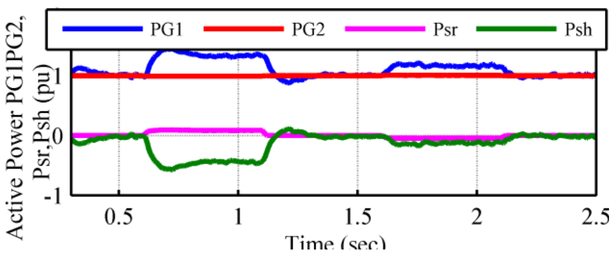

Fig. 8.a Real power transfer using PI controllers

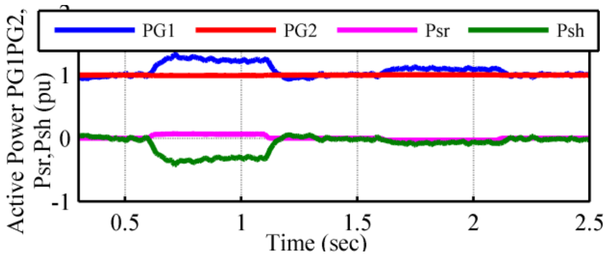

Fig. 8.b Real power transfer using NN controllers

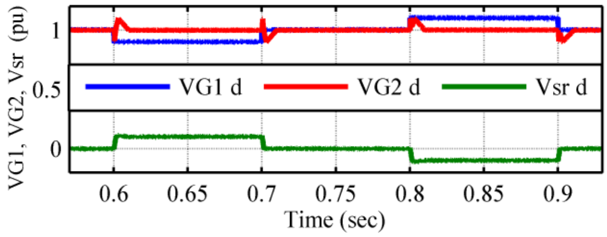

Fig. 9.a Compensation of positive sequence voltage in d axis using PI controller

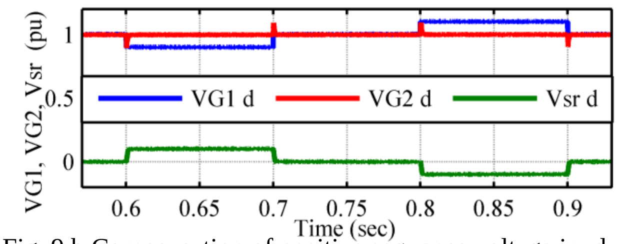

Fig. 9.b Compensation of positive sequence voltage in d axis using NN controller

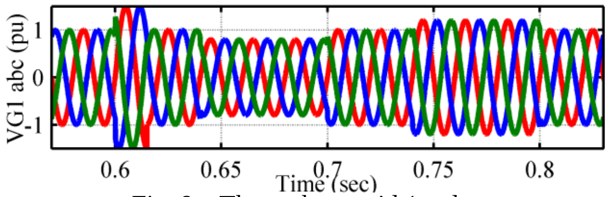

Fig. 9.c Three phase grid 1 voltage

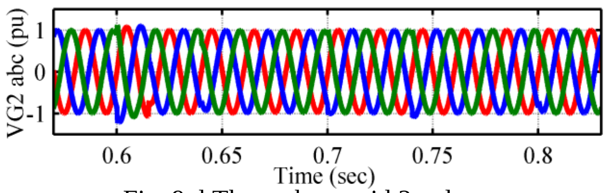

Fig. 9.d Three phase grid 2 voltage

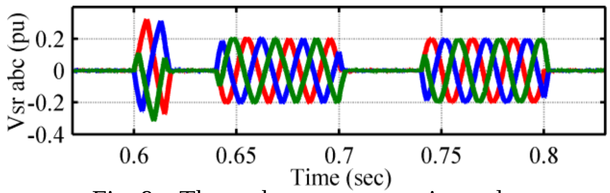

Fig. 9.e Three phase compensation voltage

6.3 Analyze on compensation of voltage at point of common coupling

This section demonstrates regulation of rated voltage of 230 KV at point of common coupling using PI controller and NN controller. The simulation results of regulation of positive sequence voltage V_{G1}, V_{G2} and V_{sr} in d axis using PI controller and NN controller are shown in Fig. 9.a and Fig. 9.b respectively. 10% under voltage is introduced between 0.6 sec to 0.7 sec and 10% of over voltage is injected at V_{G1} from 0.8 sec to 0.9 sec. The main objective of the proposed configuration is to maintain rate voltage 230KV at point of common coupling. Under normal operating conditions, V_{G1} and V_{G2} are in equal and V_{sr} is found to be zero. For under voltage condition, required voltage is injected by series VSI and thereby rated voltage is maintained at point of common coupling. For over voltage condition, required voltage is absorbed by series VSI and thereby rated voltage is maintained. While using PI controller, transient detection is found to be poor and it requires more time to compensate whereas using NN controller, transient detection is found to be optimum and it has fast compensation time. This analyzes are clearly projected in Fig. 9.a and Fig. 9.b. respective. The simulation results for three phase voltage of grid 1, grid 2 and series voltage or compensation voltage are shown in Fig. 9.c, Fig. 9.d and Fig. 9.e respectively. Under normal condition, rated voltage is maintained whereas under faulted condition the require voltage is injected by the series VSI such that it maintains rated voltage at grid 2.

7. Conclusion

A neural network DQ control technique based UHVDC is proposed for the management of transient and fast power transfer between offshore WPP and onshore electric grid. The performance of the proposed neural network control scheme is investigated under disturbances in both WPP and electric grids and compared with PI controller. From the test results, it is found that neural network based control technique has better capability to compensate transients and superior power transfer between WPP and power grid.

References

1. Moawwad, M., Shawky E.I., Moursi, Weidong X.: *A Novel control strategy for VSC-HVDC connecting offshore wind power plant*. In: IEEE Trans. Sustain. Ener., vol. 5, no.3, pp. 1204–1212, Jun. 2014.
2. Bresesti P., Kling W. L., Hendriks R. L., Vailati R.: *HVDC connection of offshore wind farms to the transmission system*. In: IEEE Trans. Energy Convers., vol. 22, no. 1, pp. 37–43, Mar. 2007.
3. Flourentzou N., Agelidis V., Demetriades G.: *VSC-based HVDC power transmission systems: An overview*. In: IEEE Trans. Power Electron, vol. 24, no. 3, pp. 592–602, Mar. 2009.
4. Alvarez E., Bianchi F., Ferre A.J.:, Gross G., Bellmunt O.G.: *Voltage control of multi terminal VSC-HVDC transmission systems for offshore wind power plants: Design and implementation in a scaled platform. In:* IEEE Trans. Ind. Electron., vol. 60, no. 6, pp. 2381–2391, Jun. 2013.

Table 1 Performance comparison of PI and controllers

Operation Condition	DC link Voltage Control				Time taken for Transient Compensation (msec)	
	Peak Overshoot (%)		Settling Time (msec)		PI	NN
	PI	NN	PI	NN		
Initial condition	18.3	1.41	450	380	600	450
WPP side disturbances	11	5	160	100	250	100
Grid Side Disturbances	20.5	4	500	250	280	110

Table 2 System parameter

Electric Grids		Offshore Station	
Frequency	50Hz	Rated Power	250MVA
Grid voltage	230KV	WPP Voltage	33KV
X/R	20	Transformer Ratio	33KV/230KV
Short circuit ratio	30	Leakage Reactance	0.11pu
Leakage Reactance	0.11pu	AC Filter L1	40mf
Transmission Line Impedance	0.2pu	AC Filter C1	100uf
Onshore Station			
Series Compensator		Shunt Compensator	
Rated Power	125MVa	Rated Power	125MVa
Transformer rating	200MVA	Transformer rating	200MVA
TRANSFORMER Leakage reactance	0.06pu	TRANSFORMER Leakage reactance	0.11pu
AC Filter 2 Series L2s	20mh	AC Filter 2 Series L2s	45mh
AC Filter 2 Series C2s	100uF	AC Filter 2 Series C2s	150uF
DC Link			
DC Link Voltage		400KV	
DC Capacitance		1600uF	
DC cable resistance		0.004ohms/km	
DC cable capacitances		11.3uF/km	

5. Narayanan N.K., Mitra P.: *A Comparative Study of a Sequential and Simultaneous AC-DC Power Flow Algorithms for a Multi-Terminal VSC-HVDC System*. In: Innovative Smart Grid Technologies conference, Bangalore, India, Nov. 2013.
6. Feng W., Tuan L.A., Tjernberg L.B., Mannikoff A., Bergman A.: *A New Approach for Benefit Evaluation of Multiterminal VSC–HVDC Using A Proposed Mixed AC/DC Optimal Power Flow*. In: IEEE Trans. Power Del., vol. 29, no. 1, pp. 432-443, Feb. 2014.
7. Alepuz S. et al., "*Control strategies based on symmetrical components for grid-connected converters under voltage dips*," IEEE Trans. Ind. Electron., vol. 56, no. 6, pp. 2162–2173, Jun. 2009.
8. Adam G.P., Ahmed K.H., Finney S.J., Bell K., Williams B.W.: *New breed of network fault-tolerant voltage-source-converter HVDC transmission system*. IN: IEEE Trans. Power Syst., vol. 28, pp. 335–346, Feb. 2013.
9. Huang P.H., Moursi M.E., Xiao W., Kirtley J.: *Novel fault ride through configuration and transient management scheme for doubly fed induction generator*. In: IEEE Trans. Energy Conv., vol. 28, no. 1, pp. 86–94, Mar. 2013.
10. Pinto et R.T. al.: *A novel distributed direct-voltage control strategy for grid integration of offshore wind energy systems through MTDC network*. In: IEEE Trans. Ind. Electron., vol. 60, no. 6, pp. 2429–2441, Jun. 2013.
11. Chaudhary S.K., Teodorescu R., Rodriguez P., Kjaer P.C., Gole A.M.: *Negative sequence current control in wind power plants with VSC-HVDC Connection*. In: IEEE Trans. Sustain. Energy, vol. 3, no. 3, pp. 535–544, Jul. 2012.
12. Hingorani N.G., Gyugyi L., Hawary M.E.: *Understanding FACTS: Concepts and Technology of Flexible AC Transmission Systems.* New York, NY, USA: IEEE, 2000.
13. Pinares G., Bongiorno M.: *Modeling and analysis of VSC-based HVDC system for DC network stability studie*s. In: IEEE Trans. Power Del., vol. 31, no. 2, pp. 848–857, April 2016.
14. Chen Z., Guerrero J., Blaabjerg F.: *A review of the state of the art of power electronics for wind turbines*. In: IEEE Trans. Power Electron., vol. 24, no. 8, pp. 1859–1875, Aug. 2009.
15. Baradar M., M. Ghandhari.: *A multi-option unified power flow approach for hybrid AC/DC grids incorporating multi-terminal VSC HVDC*. In: IEEE Trans. Power Syst., vol. 28, no. 3, pp. 2376-2383, Aug 2013.
16. Roiu D., Bojoi R.I., Limongi L.R., Tenconi A.: *New stationary frame control scheme for three-phase PWM rectifiers under unbalanced voltage dips conditions*. In: IEEE Trans. Ind. Appl., vol. 46, no. 1, pp. 268–277, Jan./Feb. 2010.
17. Du C., Bollen M.H.J., Agneholm E., Sannino A.: *A new control strategy of a VSC–HVDC system for high-quality supply of industrial plants*. In: IEEE Trans. Power Del., vol. 22, no. 4, pp. 2386–2394, Oct. 2007.
18. Moawwad A., Shawky M., Moursi E.I., Xiao W.: *Novel configuration and transient management strategy for VSC-HVDC*. In: IEEE Trans. Power Syst., vol. 29, no.5 pp. 2478–2488, 2014.
19. Singh B., Arya S.R., *Back-propagation control algorithm for power quality improvement using DSTATCOM*. In: IEEE Trans. Indus. Elec., vol. 61, no. 3, pp. 1204–1212, 2014.
20. Singh B., Verma V., Solanki J.: *Neural network-based selective compensation of current quality problems in distribution system*. In: IEEE Trans. Indus. Elect., vol. 54, no. 1, pp.53–60, 2007.
21. Wu J., Li , Wang G., Liang Y.: *An Improved Traveling-Wave Protection Scheme for LCC-HVDC Transmission Lines*. In: IEEE Trans. Power Del., vol. 32, no. 1, pp. 106-116, Feb. 2017.
22. Stamatiou G., Bongiorno M.: *Power-dependent droop-based control strategy for multi-terminal HVDC transmission grids*. In: IET Gen., Tran. & Dist., vol. 11, no. 2, pp. 383-391, 2017.
23. Bucher M.A., Ortega-Vazquez M.A., Kirschen D.S., Andersson G.: Robust allocation of reserves considering different reserve types and the flexibility from HVDC. In: IET Generation, Transmission & Distribution, vol. 11, no. 6, pp. 1472-1478, 2017.
24. Wang D., Lu T., Li Q., Chen B., Li X.: 3-D Electric Field Computation of Steeple Rooftop Houses Near HVDC Transmission Lines. In. IEEE Trans. Magnetics, vol. 53, no. 6, pp. 1-4, Jun. 2017
25. Hu Y. et al.: *Fault-Tolerant Converter With a Modular Structure for HVDC Power Transmitting Applications*. In: IEEE Trans. Ind. App., vol. 53, no. 3, pp. 2245-2256, May-June 2017.
26. Rouzbehi K., Zhang W., Candela J.I., Luna A., Rodriguez P.: Unified reference controller for flexible primary control and inertia sharing in multi-terminal voltage source converter-HVDC grids. In: IET Gen., Tran. & Dist., vol. 11, no. 3, pp. 750-758, Feb. 2017
27. Schönleber K., Collados C., Pinto R.T., Palau S.R., Bellmunt O.G.: *Optimization-based reactive power control in HVDC-connected wind power plants*. In: Renewable Energy, vol. 109, pp. 245-260, Aug. 2017.
28. Alam M.M, Leite H., Liang J., Carvalho A.S.: *Effects of VSC based HVDC system on distance protection of transmission lines*. In: International Journal of Electrical Power & Energy Systems, vol 92, pp. 500-509, Nov. 2017.
29. Alvarez A.E., Penalba M.A., Araujo E.P., Bellmunt O.G.: *Power reduction coordinated scheme for wind power plants connected with VSC-HVDC*. In: Renewable Energy, vol. 107, pp. 1-13, Jul. 2017.
30. Yang Q, Blond S.L., Aggarwal R., Wang Y., Li J.: *New ANN method for multi-terminal HVDC protection relaying*. In: Electric Power Systems Research, vol. 148, pp. 192-201 Jul. 2017.